

DENSE CLOUD ABLATION AND RAM PRESSURE STRIPPING OF THE VIRGO SPIRAL NGC 4402

HUGH H. CROWL AND JEFFREY D. P. KENNEY

Astronomy Department, Yale University, P.O. Box 208101, New Haven, CT 06520;
 hugh@astro.yale.edu, kenney@astro.yale.edu

J. H. VAN GORKOM

Department of Astronomy, Columbia University, 538 West 120th Street, New York, NY 10027;
 jvangork@astro.columbia.edu

AND

BERND VOLLMER

CDS, Observatoire Astronomique de Strasbourg, UMR 7550, 11 Rue de l'Universite, 67000 Strasbourg, France;
 bvollmer@newb6.u-strasbg.fr

Received 2004 November 5; accepted 2005 March 21

ABSTRACT

We present optical, H I, and radio continuum observations of the highly inclined Virgo Cluster Sc galaxy NGC 4402, which show evidence for ram pressure stripping and dense cloud ablation. Very Large Array H I and radio continuum maps show a truncated gas disk and emission to the northwest of the main disk emission. In particular, the radio continuum emission is asymmetrically extended to the north and skewed to the west. The H α image shows numerous H II complexes along the southern edge of the gas disk, possibly indicating star formation triggered by the intracluster medium (ICM) pressure. Our *BVR* images at 0".5 resolution obtained with the WIYN Tip-Tilt Imager show a remarkable dust lane morphology: at half the optical radius, the dust lane of the galaxy curves up and out of the disk, matching the H I morphology. Large dust plumes extend upward for ~ 1.5 kpc from luminous young star clusters at the southeast edge of the truncated gas disk. These star clusters are very blue, indicating very little dust reddening, which suggests dust blown away by an ICM wind at the leading edge of the interaction. To the south of the main ridge of interstellar material, where the galaxy is relatively clean of gas and dust, we have discovered 1 kpc long linear dust filaments with a position angle that matches the extraplanar radio continuum tail; we interpret this angle as the projected ICM wind direction. One of the observed dust filaments has an H II region at its head. We interpret these dust filaments as large, dense clouds that were initially left behind as the low-density interstellar medium was stripped but were then ablated by the ICM wind. These results provide striking new evidence on the fate of molecular clouds in stripped cluster galaxies.

Key words: galaxies: clusters: general — galaxies: clusters: individual (Virgo) — galaxies: evolution — galaxies: ISM — galaxies: peculiar

1. INTRODUCTION

The morphology-density relationship (Oemler 1974; Melnick & Sargent 1977; Dressler et al. 1997) is one of the clearest examples of the effect that clusters have on their member galaxies. There are several cluster processes that may contribute to this observed effect (Treu et al. 2003). Mergers, harassment (repeated high-speed galaxy-galaxy interactions), and tidal truncation of the outer galactic regions by the cluster potential (Merritt 1984; Natarajan et al. 2002) are among the suggested gravitational effects for galactic morphological transformation in clusters. The effects of the intracluster medium (ICM) on the galactic interstellar medium (ISM) include ram pressure stripping (Gunn & Gott 1972; Abadi et al. 1999), turbulent and viscous stripping (Nulsen 1982; Toniazzo & Schindler 2001), and the thermal evaporation of the ISM by the hot ICM (Cowie & Songaila 1977). It is believed that ISM-ICM stripping (which includes both ram pressure stripping and turbulent viscous stripping) may be among the most important processes in the transformation of late-type cluster spirals into Sa and S0 galaxies. This process, which removes gas from the galaxy but leaves the stars unperturbed, results in galaxies with truncated gas and star-forming disks (Warmels 1988; Cayatte et al. 1990; Koopmann & Kenney 2004a, 2004b). Simulations of ISM-ICM

interactions (e.g., Quilis et al. 2000; Schulz & Struck 2001; Vollmer et al. 2001) have shown that a smooth, uniform ISM can be stripped from the outer regions of galaxies in clusters via ram pressure. However, such simulations necessarily assume an overly simplistic ISM and, hence, are unable to model the multiphase ISM as it exists in spiral galaxies. In particular, the fate of star-forming molecular clouds must be known in order to fully understand how stripping affects cluster galaxy evolution. Studying the details of an ISM-ICM interaction can help us learn what role gas stripping plays in the morphology-density relation. There is abundant evidence that NGC 4402 is undergoing such an interaction.

NGC 4402 is an H I-deficient, $0.3L_*$ Sc galaxy located near the center of the Virgo Cluster, $1^\circ 4'$ (390 kpc projected) from the giant elliptical galaxy M87. It is also the nearest spiral galaxy to the giant elliptical galaxy M86, making it plausible that this galaxy is associated with the M86 subcluster (Schindler et al. 1999). NGC 4402 is highly inclined ($i = 80^\circ \pm 3^\circ$), making it possible to distinguish stripped extraplanar gas from disk gas. Its line-of-sight velocity of 237 km s^{-1} (Rubin et al. 1999) means that it is blueshifted relative to the mean cluster velocity by nearly 800 km s^{-1} . This, in turn, means that the near side of the galaxy contains the leading edge of the ISM-ICM interaction, allowing us to observe key details of the ISM-ICM

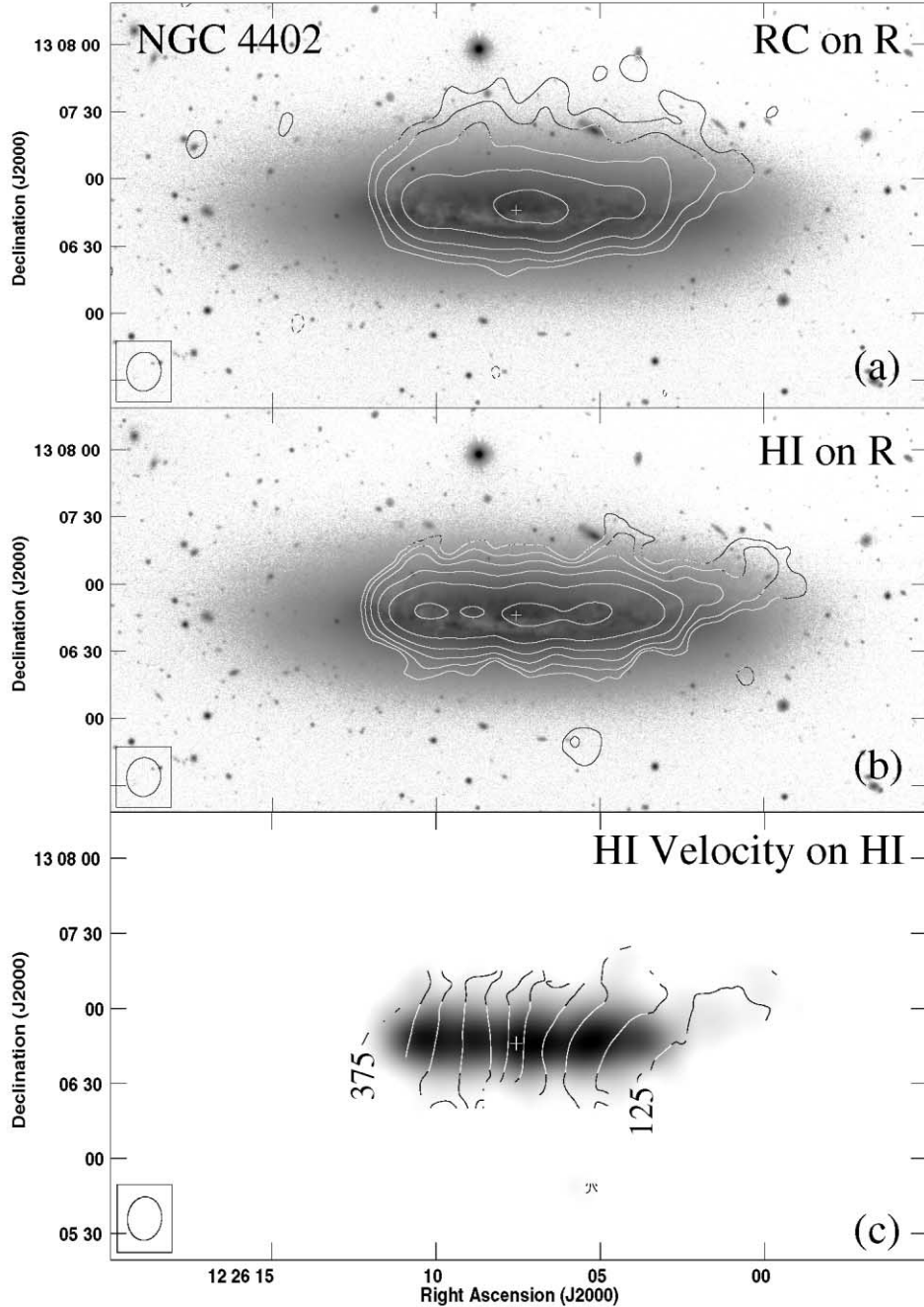


FIG. 1.—(a) 1.4 GHz radio continuum contours overlaid on a MiniMosaic *R*-band image. The contours are $-0.46 \text{ mJy beam}^{-1}$ and range from 0.46 to 14 mJy beam^{-1} by factors of 2. The *R* image is shown in a logarithmic stretch; R_{25} is located approximately 1.7 times farther out than the lowest contour level. (b) H I contours on the *R*-band image. Contours range from $0.6 M_{\odot} \text{ pc}^{-2} = 8 \times 10^{19} \text{ cm}^{-2}$ to $19.2 M_{\odot} \text{ pc}^{-2} = 2.6 \times 10^{21} \text{ cm}^{-2}$ by factors of 2. (c) H I velocity contours on H I gray scale. Contours range from 125 km s^{-1} in the west to 375 km s^{-1} in the east and are incremented by 25 km s^{-1} .

stripping in this galaxy. In this paper, we present new high-resolution ($0''.5$) optical images, along with 21 cm Very Large Array (VLA) radio maps of NGC 4402. We show that both the radio and optical data provide a strong constraint on the ICM wind direction and that the optical data suggest dense cloud ablation by the ICM wind. Although present millimeter interferometers do not have the sensitivity or resolution to show what happens to giant molecular clouds in stripped galaxies, the high-resolution optical images of star formation and dust extinction suggest what may happen to large dense gas clouds in NGC 4402.

2. OBSERVATIONS

2.1. Radio Data

NGC 4402 was observed with the VLA¹ in the C configuration in 2003 January as part of a study of four edge-on spiral galaxies in the Virgo Cluster. We used the 21 cm spectral line mode with online Hanning smoothing and the system tuned

¹ The VLA is operated by the National Radio Astronomy Observatory, which is a facility of the National Science Foundation, operated under cooperative agreement by Associated Universities, Inc.

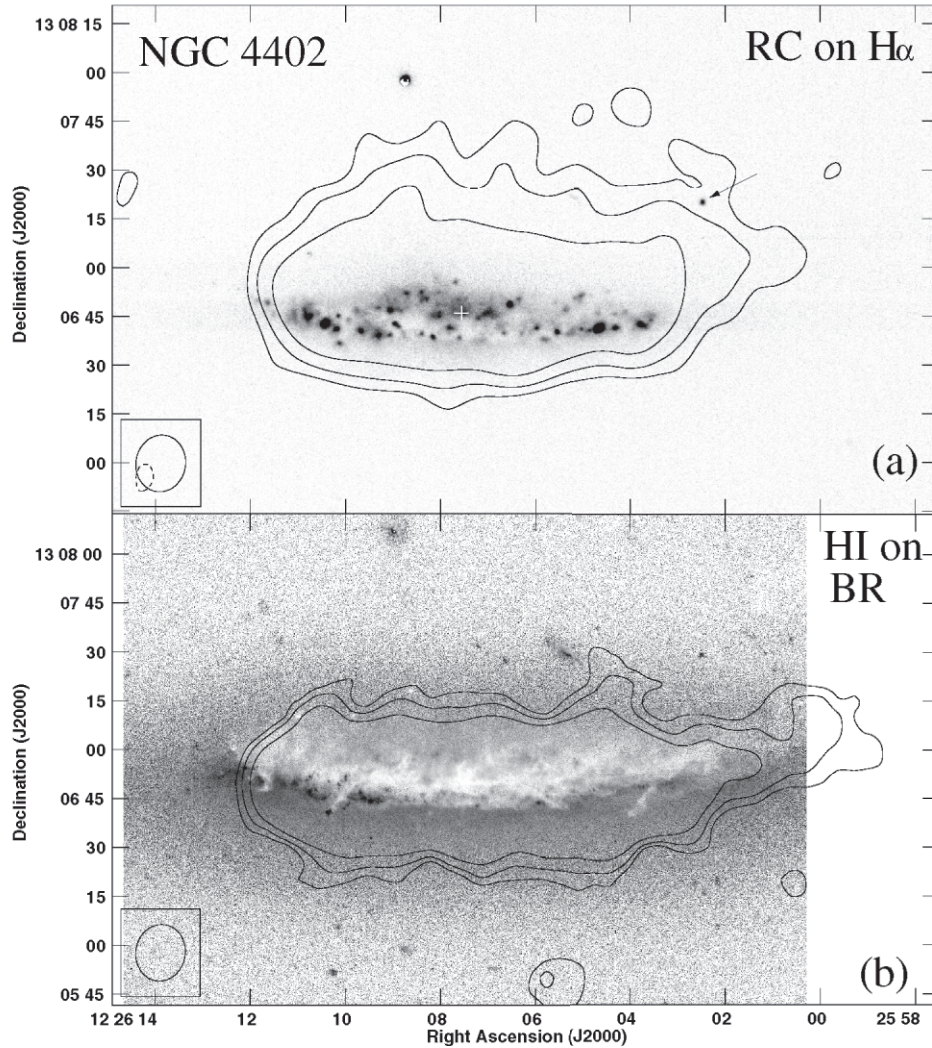


FIG. 2.—(a) $H\alpha$ image showing the outer three radio continuum contours. The extraplanar $H\text{ II}$ region from Cortese et al. (2004) is marked with an arrow. (b) $B - R$ image from WTTM images showing dust lane detail in the galaxy, along with the outer three $H\text{ I}$ contours. Note the very blue star clusters in the southeast, probably due to minimal reddening by dust.

to a central velocity of 200 km s^{-1} . In this configuration, the system has a bandwidth of 3.125 MHz and 63 channels, each with a width of 10.4 km s^{-1} . The data were calibrated, mapped, and CLEANed in AIPS using standard techniques and procedures. Maps were made with the IMAGR task with a ROBUST weighting parameter of +1, resulting in a beam size of $17''.4 \times 15''.2$ ($\sim 1.2 \text{ kpc}$, assuming a distance of 16 Mpc). Thirty of the channels show $H\text{ I}$ emission at the $>3\sigma$ level (where $\sigma = 0.32 \text{ mJy beam}^{-1}$). These channels were combined to make moment maps of the $H\text{ I}$ emission. Fifteen line-free channels were combined to make the continuum map. Maps of the total $H\text{ I}$ emission and radio continuum emission are shown in Figure 1. We detect a total $H\text{ I}$ flux of $6.50 \pm 0.55 \text{ Jy km s}^{-1}$. This compares with an average single-dish $H\text{ I}$ flux in the literature of $7.16 \pm 0.70 \text{ Jy km s}^{-1}$ (Giovanelli & Haynes 1983; Helou et al. 1984; Giovanardi & Salpeter 1985), suggesting that there is no significant flux missing in our interferometer observations. The $H\text{ I}$ mass of this galaxy as measured from our data is $3.9 \times 10^8 M_{\odot}$. This galaxy is moderately $H\text{ I}$ deficient, with a deficiency parameter of 0.61 (Giovanelli & Haynes 1983), roughly 25% of the “normal” $H\text{ I}$ content for a galaxy in a low-density environment.

2.2. Optical Imaging Data

The optical data were taken during two separate observing runs at the WIYN telescope.² The high-resolution imaging data were taken over two nights in 2004 March using the WIYN Tip-Tilt Module (WTTM) on the WIYN 3.5 m telescope. The WTTM is a first-order adaptive optics system that allows us to correct the already excellent seeing at WIYN by $0''.1$ – $0''.15$ through use of a bright guide star (Claver et al. 2003). As a result we were able to obtain B , V , and R images with $0''.5$ seeing. The deep R and narrowband $H\alpha$ images were taken in 2000 April at WIYN using the MiniMosaic imager. The resulting images have an average seeing of approximately $1''$. For both data sets, standard IRAF image reduction tasks were used to bias-correct, flat-field, and combine the images. The R -band image was used to subtract the continuum emission from the $H\alpha$ narrowband image and produce an $H\alpha + [\text{N II}]$ image. The MiniMosaic R and $H\alpha$ images are shown in gray scale in Figures 1 and 2a,

² The WIYN Observatory is a joint facility of the University of Wisconsin—Madison, Indiana University, Yale University, and the National Optical Astronomy Observatory.

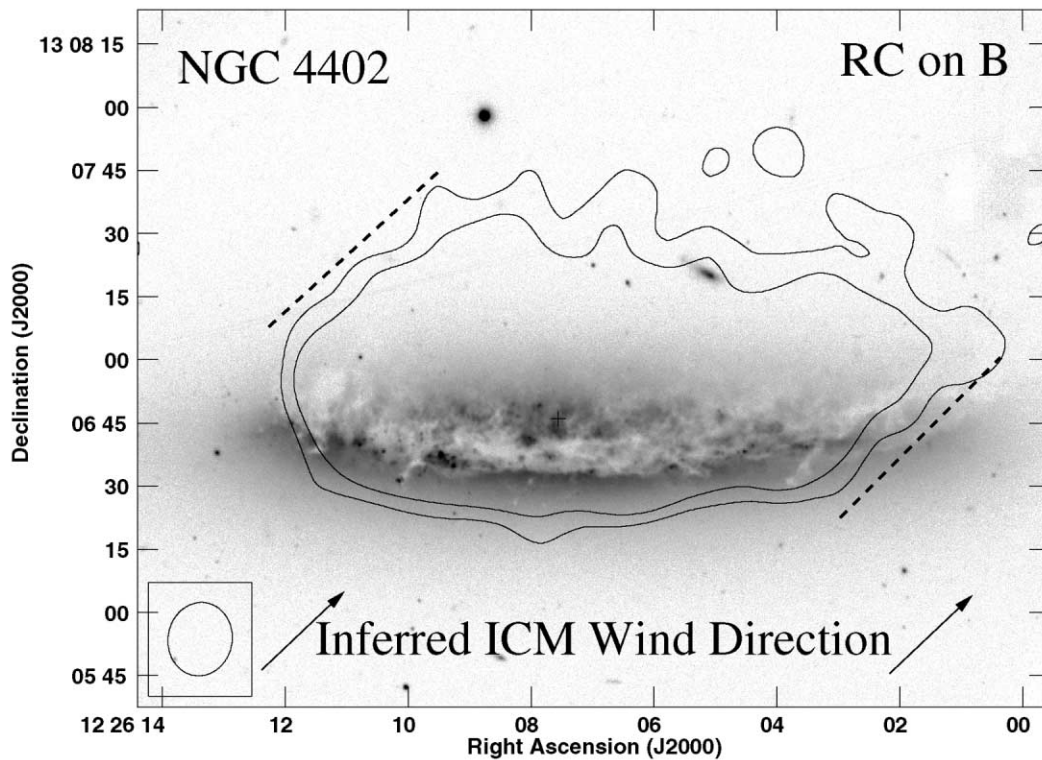


FIG. 3.—Outer two 1.4 GHz radio continuum contours on the WTTM *B* image. The dashed lines indicate the “sharp ridges with well-determined position angles” discussed in the text. The inferred projected ICM wind direction (P.A. = -43°), as calculated from the average of the position angles of the filaments and of the radio continuum ridges, is indicated with arrows at the bottom of the image.

together with the H I and radio continuum contour maps. A higher resolution WTTM *B* – *R* image is shown in Figure 2*b*, and a color version of the higher resolution *BVR* image is shown in Figure 4 (discussed further below).

3. RESULTS

The stellar disk appears undisturbed, since the outer isophotes of the *R*-band image are elliptical, concentric, and at a constant position angle. Within the disk, both the H I and radio continuum (Figs. 1*a* and 1*b*) are truncated (i.e., no emission at a 2σ level) at $0.6\text{--}0.7R_{25}(=70''\text{--}82'' = 5.4\text{--}6.4\text{ kpc})$, demonstrating that the undisturbed stellar disk extends well beyond the location of the gas. Throughout the part of the disk still containing H I and radio continuum emission, heavy dust lanes are evident (Fig. 2*b*).

The truncation radius is similar for the H I and radio continuum on the eastern edge of the galaxy ($\sim 0.6R_{25}$) but more complicated in the west. If one considers only the symmetric disk components, the radio continuum and H I emission both extend to $\sim 0.7R_{25}$ along the major axis in the west. However, there is a component of the radio continuum halo north of the major axis that extends to $0.9R_{25}$ and a significant component of the H I emission north of the major axis that extends to $1.1R_{25}$. The apparent extraplanar emission in both the H I and radio continuum maps is displaced to the northwest of the disk emission, consistent with an ICM wind acting from the southeast direction, although the distributions of extraplanar emission differ. While there are many processes that may drive galactic evolution in clusters, ICM-ISM stripping is the only one that can asymmetrically strip the gas from the outer parts of a galaxy without disturbing the stars.

The radio continuum emission is asymmetrically extended away from the disk midplane. South of the major axis, the radio continuum contours are compressed, consistent with a margin-

ally resolved or unresolved distribution. In contrast, north of the major axis, the radio continuum contours are stretched out, reaching at least $60''$ (500 pc) to the north of the disk. North of the major axis, there is a 50% excess of radio continuum emission compared to the emission from south of the major axis. Many edge-on galaxies are observed to have extended radio continuum halos, both inside and outside of clusters (Irwin et al. 1999). The causes of these extended halos are not well understood but are likely related to the star-forming activity in the disk. Since 25% of the edge-on galaxies in the Irwin et al. (1999) sample are observed to have larger radio continuum extents than that of NGC 4402, we cannot say with certainty that the large extent of the northern radio continuum halo is due to the ICM wind. However, what is clearly unusual about the radio continuum halo in NGC 4402 is the large asymmetry on the two sides of the major axis and a clear skewing of the northern radio continuum halo toward the northwest. Figures 1*a* and 3 show that the two sides of the radio continuum tail form fairly sharp ridges with well-determined position angles of -49° (east) and -47° (west). These relatively sharp boundaries may be indicative of the projected ICM wind direction. No other edge-on galaxy in the Irwin et al. (1999) sample shows such an asymmetry or skew.

The H I map (Fig. 1*b*) shows two possible extraplanar features: a small one $50''$ (3.9 kpc) west and $40''$ (3.1 kpc) north of the nucleus, apparently lying above the main disk H I emission, and a larger curved feature extending for 0.8 beyond the western disk truncation radius, lying $25''$ north of the major axis. The velocity structure of these components can be seen in the moment 1 map (Fig. 1*c*). The gas to the north of the disk has a higher line-of-sight velocity (and lower galactocentric velocity) by $\sim 20\text{ km s}^{-1}$ than the corresponding disk gas along the major axis. We can put an upper limit on the amount of extraplanar H I by assuming the disk emission is symmetric

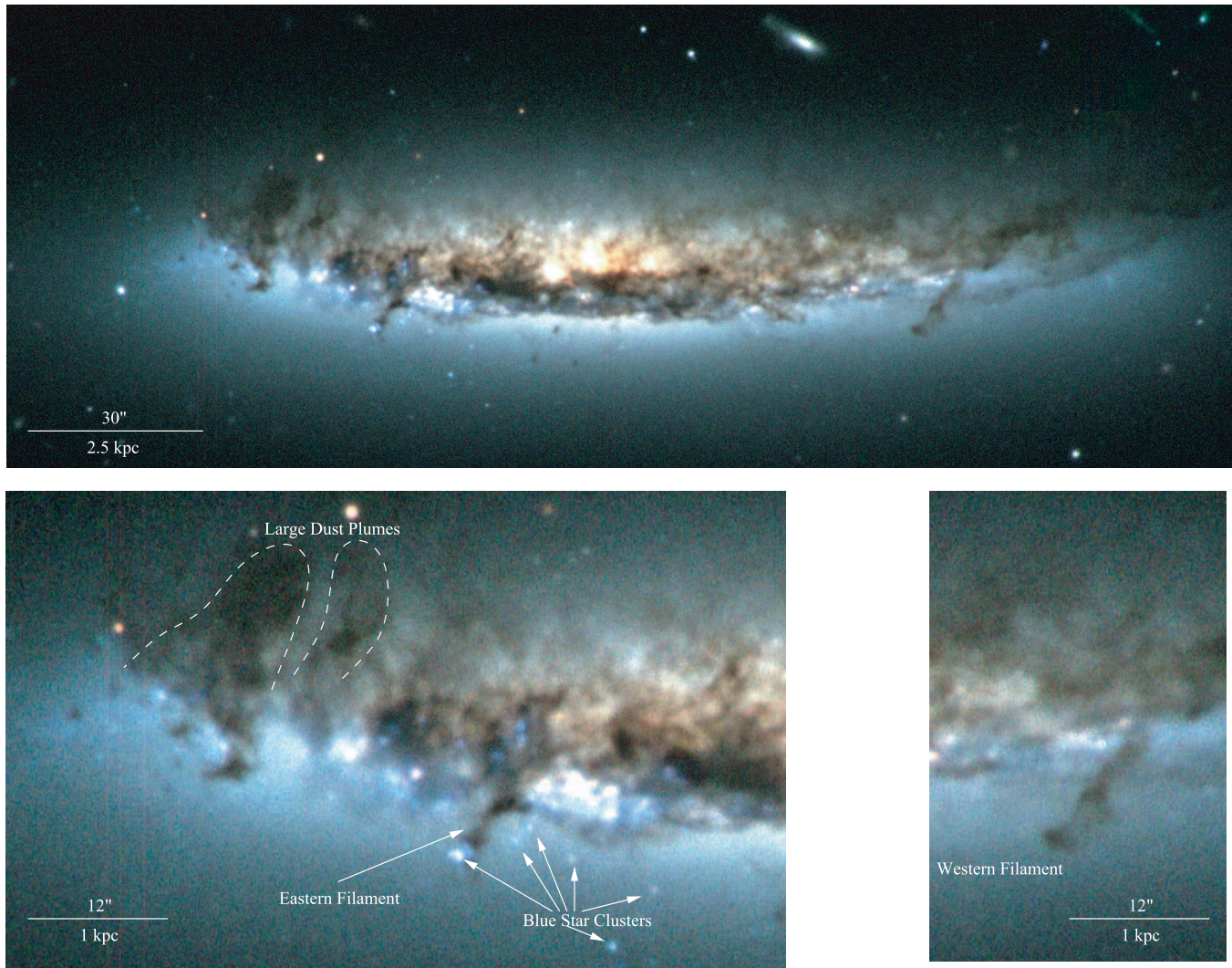


Fig. 4.—*BVR* color image (top) of NGC 4402, with detail images of the western filament (bottom right) and eastern filament and blue star clusters (bottom left).

about the major axis and subtracting a disk component from regions north of the major axis. Approximately 6% of the total $H\ I$ flux ($0.40\ \text{Jy km s}^{-1}$) is outside of the symmetric disk, corresponding to $2.4 \times 10^7\ M_{\odot}$. This “extraplanar” $H\ I$ fraction and mass are much lower than the 40% and $1.5 \times 10^8\ M_{\odot}$ detected in the highly inclined Virgo spiral NGC 4522 (Kenney et al. 2004), a good candidate for ongoing stripping. The 6% excess of $H\ I$ flux is also significantly lower than the 50% excess of radio continuum emission north of the major axis in NGC 4402.

The total $H\alpha$ luminosity of the galaxy is $7.9 \times 10^{40}\ \text{ergs s}^{-1}$, which corresponds to a star formation rate (SFR) of $0.6\ M_{\odot}\ \text{yr}^{-1}$, whereas the far-infrared (FIR) luminosity from *IRAS* fluxes (Soifer et al. 1989) corresponds to an SFR of $1.2\ M_{\odot}\ \text{yr}^{-1}$. The FIR-based SFR is unsurprisingly higher for this dusty, highly inclined galaxy, but the $H\alpha$ image still shows a large fraction of the star formation activity in the galaxy. The $H\alpha$ emission (Fig. 2a) is strong along the southern edge of the galaxy. Asymmetric $H\alpha$ enhancements at the gas truncation radius have been observed in other galaxies in Virgo and other clusters (Koopmann & Kenney 2004b; Vogt et al. 2004) and interpreted as a sign of ongoing pressure. $H\alpha$ emission from star-forming complexes is strong in both the southeast and southwest, but the complexes in the southeast are much bluer in the $B - R$ and color images (Figs. 2b and 4). It appears that the southeast star clusters

suffer less dust reddening and extinction because the ICM wind has pushed away much of the dust at the leading edge of the galaxy, an interpretation supported by the dust plumes extending upward from the southeast star-forming regions. This provides evidence that the southeast region, opposite the northwest radio continuum tail, is the leading edge of the interaction.

Our $H\alpha$ image (Fig. 2a) also shows the recently discovered extraplanar $H\ II$ region northwest of the main disk (Cortese et al. 2004), which likely formed from stripped gas. This $H\ II$ region is located within the extraplanar radio continuum tail and close to, but not coincident with, the “extraplanar” $H\ I$. Approximately 0.3% of the total $H\alpha$ luminosity is from this extraplanar $H\ II$ region, much lower than the extraplanar $H\alpha$ fraction of 10% in NGC 4522 (Kenney et al. 2004).

The $H\ I$ and radio continuum distributions are different, indicating that they trace different components of the ISM. $H\ I$ emission traces the warm, neutral medium, and nonthermal radio continuum emission traces relativistic electrons spiraling in magnetic fields, perhaps produced by supernovae resulting from recent star formation. The $H\ I$ is more extended than the radio continuum along the major axis in the west. This could simply be the result of the low radio continuum-to- $H\ I$ ratio generally observed in the outer disks of spirals, due to the low efficiency of outer disk $H\ I$ in forming stars (Kennicutt 1989).

Consequently, there are few products of star formation, including radio continuum emission, in outer disk gas. Figure 2a shows that the radio continuum emission in the disk is co-extensive with regions of star formation along the major axis, and that the westernmost H I has no associated H II regions. In the north, the radio continuum emission is more extended than the H I along the minor axis, as discussed below.

The high-resolution images of the dust lanes seen in the $B - R$ image (Fig. 2b) and BVR color image (Fig. 4) are especially striking. The strongest dust lanes are across the southern part of the stellar disk, indicating that the southern side of the galaxy is the near side. The color image (Fig. 4) shows that the galaxy starlight south of the main dust band is relatively blue, while in the north it is significantly reddened by the displaced dust. This is the *opposite* of what is normally observed in undisturbed galaxies, in which the near side of the galaxy appears to be more reddened. The BVR and $B - R$ images show a fairly well-defined boundary between the region of NGC 4402 that still contains large amounts of dust and the region that has been swept mostly clean. There are very few dust extinction features observed south of the main boundary. While dust is an excellent ISM tracer, we can only observe it via optical extinction if the dust is in front of most of the stars. Therefore, the lack of dust extinction features south of the main truncation boundary indicates that there is very little dust above or near the midplane of the outer southern stellar disk. Heavy dust lanes are evident throughout that part of the disk still containing H I and radio continuum emission. In both the east and the west, at the H I truncation radii, the dust lanes curve upward and away from the plane of the stellar disk. The departure from the disk is more gradual in the west and more pronounced in the east, similar to the radio continuum and H I distributions. In the east-southeast, which we think may be the leading edge of the gas disk, the dust features curve upward from the luminous star-forming complexes for at least $20'' = 1.5$ kpc. The $B - R$ map (Fig. 2b) shows that the H I contours appear to cut off *inside* the dust distribution, suggesting that the less dense gas in this part of the galaxy has already been stripped.

4. DISCUSSION

The sharpness of the southern boundary in the color image (Fig. 4) reveals important information on how the multiphase ISM reacts to ICM pressure. In the H I map (Fig. 1b), the southern boundary is not smooth, but featured, perhaps because of ISM structure within the disk. The optical image shows that the region south of the main ISM boundary contains a few faint dust features and young blue star clusters. The most remarkable dust features south of this boundary are two linear dust filaments, shown in Figure 4, with widths of $\sim 1'' - 2''$ (80–150 pc) and lengths of $7''$ (0.5 kpc) and $13''$ (1.0 kpc). These two filaments have nearly the same position angle (-40° in the east and -36° in the west) and point roughly in the same direction as the radio continuum tail, indicating that their morphology is associated with the ICM wind direction. The eastern filament shows two pieces of additional evidence of dense gas. First, there is a star formation region that appears to be associated with the head of the filament. Near the eastern dust filament, there are several (~ 10) additional blue star clusters that are also south of the main truncation edge. Second, there is a weak feature in the H I map possibly associated with that filament. We can estimate lower limits on the gas column densities, N_H , and gas masses of these filaments using the relative extinction of dust features (Howk & Savage 1997). The eastern dust filament has an average relative extinction of $a_V = 0.27$

over an area of 6.5 arcsec^2 ($4.0 \times 10^4 \text{ pc}^2$), and the western filament has an average relative extinction of $a_V = 0.13$ over an area of 13 arcsec^2 ($8.1 \times 10^4 \text{ pc}^2$). Assuming a ratio of total-to-selective absorption of $R_V = 3.6$, and using the method of Howk & Savage (1997), we find that both the eastern and western dust filaments have $M_{\text{gas}} > 2 \times 10^5 M_\odot$. This is a strict lower limit, since foreground stars (which are numerous if the filament head is near the disk midplane) and small dense lumps in the filaments can cause us to underestimate the extinction, making the true cloud mass higher.

Extraplanar dust filaments have been observed in many galaxies both inside and outside of galaxy clusters (Howk & Savage 1999; Alton et al. 2000). In many cases, these filaments are associated with fountains of gas and dust driven by star formation in the disk. In NGC 4402, there are several different types of dust features observed. The most prominent, perhaps, is the large plume of dust (with dimensions $15'' \times 6'' = 1.3 \text{ kpc} \times 0.5 \text{ kpc}$) and other dusty clumps north of the minimally reddened star clusters in the east. Once again using the method shown in Howk & Savage (1997), we can put lower limits on the mass of the two largest dust plumes (outlined in the close-up image of Fig. 4). The large plume farthest to the east has a mass of $M > 2 \times 10^6 M_\odot$, and the plume $7''$ west of it has a mass of $M > 6 \times 10^5 M_\odot$. West of the eastern dust plumes and north of the main dust band, we observe a complex filamentary structure similar to those observed in other galaxies. These structures are similar in morphology to the “irregular clouds” and “arcs” observed in NGC 891 (Howk & Savage 2000) and are likely due to star formation activity in the disk. Finally, 1.5 west of the minor axis and beyond, there are long, curved, smooth dust features. The lack of strong star formation at this location has apparently left these dust features undisturbed. The filaments observed south of the disk in NGC 4402 (described above), which we believe are *not* caused by star formation, are different in several ways. First, the two large filaments we have observed are linear. By contrast, filaments observed in other galaxies (i.e., NGC 891 and NGC 3628) and north of the disk of NGC 4402 have more complex morphologies with significant substructure and curvature and a large variety of position angles. This is the morphology that one would expect of dust ejected out from different star-forming regions and falling back to the disk via gravity. Second, there is very little dust observed in the region of the filaments south of the boundary, suggesting that the area has been swept relatively clean of the less dense dust. Finally, the filaments are aligned with each other and with the radio continuum tail.

The most straightforward interpretation of the observed southern filaments is that they are dense clouds in the disk midplane being ablated by the hot ICM wind. We propose that the southern tips of these filaments are *not* extraplanar but are the remnants of dense clouds in the disk, which has otherwise been swept mostly clear of its ISM. If this is true, then the “tails” of these filaments are extraplanar, swept up by the ICM wind. This suggests that some clouds, probably the biggest and densest giant molecular clouds, do not get stripped out together with the rest of the lower density ISM but are left behind, at least initially. Although we do not have direct evidence of molecular gas, the sizes (80–150 pc) and masses ($> 2 \times 10^5 M_\odot$) of these clouds are consistent with those of the largest giant molecular clouds in our galaxy (Dame et al. 1986) or the cores of giant molecular associations (GMAs; with typical sizes of ~ 300 pc; Vogel et al. 1988). In a typical spiral, over a small galactocentric annulus, there are very few of these largest clouds. If these are the remnants of GMAs, it is not surprising that they survived

longer than any other ISM tracer. If the observed dust clumps are GMAs/GMCs being ablated, one would expect to see head-tail features from ablation with a variety of sizes, reflecting the GMA/GMC mass spectrum. With our observations at $0''.5 = 40$ pc resolution, we can only see the most massive features. Higher resolution observations may show a continuum of structure from south to north across the disk; smaller molecular clouds may be visible at smaller galactic radii. The blue star clusters in the southeast are perhaps the remnants of these other molecular cloud cores. Calculations show that molecular clouds are too dense by at least a factor of ~ 10 to be directly stripped by ram pressure in a cluster like Virgo (Kenney & Young 1989; Kenney et al. 2004). Our observations of NGC 4402 suggest that while some clouds may survive the initial stripping, they are eventually destroyed by the ICM wind, probably aided by star formation and normal cloud evolution, which act themselves on timescales of $\sim 10^7$ yr (Larson 2003) to destroy molecular clouds. The cloud is ablated in an outside-in manner: the outer, less dense parts of the clump of material are stripped off first. This material then streams behind the clump to form a head-tail morphology. In the eastern filament, either this wind has triggered star formation or ablation has exposed an already existing star-forming region. At the leading edge of the disk, molecular clouds can probably be triggered to form stars by ISM pressure. While a fraction of the cloud mass is converted into newly formed stars, most will be returned to the lower density ISM by the destructive energy of the young stars (Larson 2003), where it can be more easily stripped.

An important parameter in systems such as NGC 4402 is the stage of the ISM-ICM interaction. In the case of NGC 4402, the optical image provides compelling evidence of an ongoing interaction. Specifically, the upward swirl of dust from minimally reddened luminous star clusters at the gas truncation radius in the southeast, the aligned linear dust filaments just beyond the gas truncation radius, and the extended and skewed radio continuum halo all strongly suggest that NGC 4402 is currently experiencing ICM pressure. This pressure is apparently strong enough to disturb the radio halo, ablate the molecular cloud cores, and push dust up into the halo of the galaxy. However, simulations of ram pressure stripping (Quilis et al. 2000; Schulz & Struck 2001; Vollmer et al. 2001) show significant amounts of extraplanar gas close to the disk in the early phases of stripping. Although 75% of the original H I is missing, there is very little extraplanar H I near the disk of NGC 4402, in contrast to NGC 4522 (Kenney et al. 2004), in which 40% of the H I is extraplanar. This result seems at odds with a near-peak ram pressure scenario. The seemingly conflicting results yield two possible explanations: (1) The galaxy is in an early phase of stripping, but the stripped extraplanar gas is no longer in the form of H I. The gas has become ionized shortly after leaving the disk so that it no longer appears in the H I phase. Indeed, heating and ionization must happen at some point, since this galaxy is quite H I deficient. If this is correct, we would expect diffuse H α and X-ray emission from this heated and ionized gas. In this scenario, the northwest radio continuum tail may be tracing the general ISM stripped from the disk of NGC 4402. (2) The galaxy is in a significantly later phase of stripping. Much of the outer disk H I has been pushed far away from the disk, but the galaxy is still experiencing pressure. If the galaxy is in a later phase of stripping, the dearth of H I is expected. In fact, this is in line with the later stages of simulations of ram pressure (Schulz & Struck 2001; Vollmer et al. 2001), which show that after ~ 100 – 500 Myr, the pressure results in a truncated gas disk with little or no extraplanar gas near the galaxy.

Other simulations (Quilis et al. 2000) have shown that viscous and turbulent stripping (Nulsen 1982) can be important over larger timescales and, therefore, may become more important than ram pressure at times following peak pressure. So, while bulk ram pressure stripping of the neutral gas may have occurred long ago, ongoing viscous and turbulent stripping may continue to strip gas from the edge of the disk well after peak pressure. In this scenario, the large vertical extent of the northern radio continuum emission does not arise from the stripping of disk gas but is a predominantly normal radio continuum halo (i.e., Irwin et al. 1999) shaped by the ICM wind, which compresses the halo in the southeast and extends it to the northwest, giving the halo its asymmetry and skew.

To determine whether our interpretations are realistic, we have made order-of-magnitude calculations of the internal pressure in the galaxy and the pressure from the ICM wind. If the radio continuum halo can be shaped by the ICM wind, the ICM wind pressure must be at least as large as the cosmic-ray energy density, as cosmic rays are the source of the radio continuum halo. Assuming a spectral index of $\alpha = -0.86$ (Vollmer et al. 2004) and measuring the radio continuum surface brightness in a small region near the truncation radius, we estimate the cosmic-ray energy density to be $u_{\text{min}}^{\text{CR}} \gtrsim 1 \times 10^{-12}$ ergs cm $^{-3}$, using the method outlined in Irwin et al. (1999). This is a lower limit of the cosmic-ray energy density, as the effective emitting volume is likely smaller than the total volume along the line of sight. The strength of the ICM wind depends on the density of the ICM and the relative velocity of the ICM and NGC 4402. From X-ray surface brightness measurements (Schindler et al. 1999), the ICM density is estimated to be $\rho_{\text{ICM}} = 5 \times 10^{-12}$ g cm $^{-3}$ at a cluster radius of $r = 0.4$ Mpc. With this density and a typical galaxy velocity of 1300 km s $^{-1}$ (Binggeli et al. 1993), the ICM ram pressure would be $\rho v^2 = P_{\text{ICM}} \sim 7 \times 10^{-12}$ dynes cm $^{-2}$. The true ram pressure could be higher or lower than this. The ICM density and, therefore, the ram pressure could be lower, since NGC 4402's clustercentric distance is probably higher than its projected distance. In contrast, the ram pressure could be higher if the ICM has bulk motions (Dupke & Bregman 2001) and the motion of the galaxy with respect to the ICM is much higher than galaxy velocity dispersions indicate (Kenney et al. 2004). Even with these uncertainties, it seems reasonable that the present ram pressure is strong enough to disturb the radio continuum halo.

The ICM pressure needed to strip neutral gas from the disk is significantly larger than that needed to disturb the radio continuum halo. The pressure needed to strip neutral gas can be estimated by considering the gravitational restoring force for a region of the galaxy (see NGC 4522; Kenney et al. 2004). Since NGC 4522 and NGC 4402 are similar in luminosity and v_{max} , it is reasonable to compare them. However, since the gas truncation radius in NGC 4402 (0.6 – $0.7R_{25} \approx 5$ kpc) is larger than that of NGC 4522 ($0.4R_{25} \approx 3$ kpc), the R -band surface brightness and the disk mass surface density at the truncation radius are lower by a factor of 2. For a gas surface density of $\sigma_{\text{gas}} = 10 M_{\odot}$ pc $^{-2}$ and an encounter angle of 45° , the gravitational restoring force per unit area is $\sigma_{\text{gas}} d\phi/dz \sim 2 \times 10^{-11}$ dynes cm $^{-2}$. This is larger by a factor of 3 than the above estimate of the ICM ram pressure for a static ICM and larger by a factor of 20 than the pressure needed to disturb the radio continuum halo. As mentioned above, turbulent viscous stripping may be an important effect that has not been considered in these simple calculations. Such effects should be most important near the edge of the galactic disk, which is where the largest disturbances of dust are observed in the optical image (Fig. 4).

Gas infall can occur either with large amounts of gas after peak pressure (Vollmer et al. 2001) or with a small amount of gas in a constant ram pressure scenario (Schulz & Struck 2001). Thus, we have considered whether the observed features, particularly the linear dust filaments, might be due to gas infalling after peak pressure. In scenarios such as these, one could, in principle, produce head-tail gas/dust features. However, an infall scenario does not easily account for the following: (1) We observed the alignment of the filaments with each other and with the radio continuum tail. If the filaments were infalling, one would expect them to fall back in the direction of the disk and galactic center and to have orientations that reflect this. In particular, the alignment of the filaments on opposite sides of the galaxy is not consistent with this and therefore not easily explained by gas fallback. (2) We observed the proximity of the southeast linear filament, with the H II region at its head, to the minimally reddened southeast disk star-forming regions and the blue star clusters. In addition, an upward swirl of dust from other star-forming complexes is evident at this location. By contrast, these observations are naturally explained by ongoing ICM pressure and dense cloud ablation.

These observations of NGC 4402 have furthered our understanding of ram pressure stripping in clusters and allowed us to question more deeply the nature of these processes. We have learned the following:

1. Not all dense clouds are strongly coupled to the lower density ISM, and it seems possible to strip low-density gas without stripping the dense clouds.

2. These dense clouds do not survive indefinitely and are eventually ablated by the ICM wind.

3. NGC 4402 is currently experiencing a wind pressure strong enough to distort the radio continuum halo and ablate the dense clouds in the disk.

However, our observations raise interesting questions on the timescales over which these processes happen. Specifically, (a) is active stripping of the neutral gas in the disk occurring now? (b) when was the outer disk of NGC 4402 stripped? and (c) on what timescales are molecular clouds destroyed by ablation? Further observations to constrain the ages of stars in the outer stellar disk may allow us to better determine the stripping history of this galaxy. Despite timescale uncertainties, it is clear that molecular clouds do not prevent the entire ISM of a galaxy from being stripped. This makes it feasible that the cessation of star formation and subsequent disk fading in cluster spirals stripped by ram pressure contributes to the transformation of these galaxies into early-type spirals and lenticulars.

We gratefully acknowledge Richard Rand for helpful discussions, Gene McDougal and the rest of the WIYN staff for effective and efficient observing support, and Mark Hanna of NOAO for assistance in the creation of a color image. We also gratefully acknowledge the referee, Curt Struck, for helpful comments that improved the paper. This research is supported by NSF grants AST 00-71251 and AST 00-98294.

REFERENCES

- Abadi, M. G., Moore, B., & Bower, R. G. 1999, *MNRAS*, 308, 947
 Alton, P. B., Rand, R. J., Xilouris, E. M., Bevan, S., Ferguson, A. M., Davies, J. I., & Bianchi, S. 2000, *A&AS*, 145, 83
 Binggeli, B., Popescu, C. C., & Tammann, G. A. 1993, *A&AS*, 98, 275
 Cayatte, V., van Gorkom, J. H., Balkowski, C., & Kotanyi, C. 1990, *AJ*, 100, 604
 Claver, C. F., Corson, C., Gomez, R. R., Jr., Daly, P. N., Dryden, D. M., & Abareshi, B. 2003, *Proc. SPIE*, 4837, 438
 Cortese, L., Gavazzi, G., Boselli, A., & Iglesias-Paramo, J. 2004, *A&A*, 416, 119
 Cowie, L. L., & Songaila, A. 1977, *Nature*, 266, 501
 Dame, T. M., Elmegreen, B. G., Cohen, R. S., & Thaddeus, P. 1986, *ApJ*, 305, 892
 Dressler, A., et al. 1997, *ApJ*, 490, 577
 Dupke, R. A., & Bregman, J. N. 2001, *ApJ*, 562, 266
 Giovanardi, C., & Salpeter, E. E. 1985, *ApJS*, 58, 623
 Giovanelli, R., & Haynes, M. P. 1983, *AJ*, 88, 881
 Gunn, J. E., & Gott, R. J. 1972, *ApJ*, 176, 1
 Helou, G., Hoffman, G. L., & Salpeter, E. E. 1984, *ApJS*, 55, 433
 Howk, J. C., & Savage, B. D. 1997, *AJ*, 114, 2463
 ———. 1999, *AJ*, 117, 2077
 ———. 2000, *AJ*, 119, 644
 Irwin, J. A., English, J., & Sorathia, B. 1999, *AJ*, 117, 2102
 Kenney, J. D. P., van Gorkom, J. H., & Vollmer, B. 2004, *AJ*, 127, 3361
 Kenney, J. D. P., & Young, J. 1989, *ApJ*, 344, 171
 Kennicutt, R. C., Jr. 1989, *ApJ*, 344, 685
 Koopmann, R. A., & Kenney, J. D. P. 2004a, *ApJ*, 613, 851
 ———. 2004b, *ApJ*, 613, 866
 Larson, R. B. 2003, *Rep. Prog. Phys.*, 66, 1651
 Melnick, J., & Sargent, W. L. W. 1977, *ApJ*, 215, 401
 Merritt, D. 1984, *ApJ*, 276, 26
 Natarajan, P., Kneib, J., & Smail, I. 2002, *ApJ*, 580, L11
 Nulsen, P. E. J. 1982, *MNRAS*, 198, 1007
 Oemler, A. 1974, *ApJ*, 194, 1
 Quilis, V., Moore, B., & Bower, R. 2000, *Science*, 288, 1617
 Rubin, V. C., Waterman, A. H., & Kenney, J. D. P. 1999, *AJ*, 118, 236
 Schindler, S., Binggeli, B., & Böhringer, H. 1999, *A&A*, 343, 420
 Schulz, S., & Struck, C. 2001, *MNRAS*, 328, 185
 Soifer, B. T., Boehmer, L., Neugebauer, G., & Sanders, D. B. 1989, *AJ*, 98, 766
 Toniazzi, T., & Schindler, S. 2001, *MNRAS*, 325, 509
 Treu, T., Ellis, R. S., Kneib, J.-P., Dressler, A., Smail, I., Czoske, O., Oemler, A., & Natarajan, P. 2003, *ApJ*, 591, 53
 Vogel, S. N., Kulikarni, S. R., & Scoville, N. Z. 1988, *Nature*, 334, 402
 Vogt, N. P., Haynes, M. P., Giovanelli, R., & Herter, T. 2004, *AJ*, 127, 3300
 Vollmer, B., Cayatte, V., Balkowski, C., & Duschl, W. J. 2001, *ApJ*, 561, 708
 Vollmer, B., Thierbach, M., & Wielebinski, R. 2004, *A&A*, 418, 1
 Warmels, R. H. 1988, *A&AS*, 72, 19